



第18届全国中高能核物理大会

QCD phase structure in the quark-meson model beyond local potential approximation

Yong-Rui Chen
June 23.2019

School of Physics
Dalian University of Technology

Based on Rui Wen, Yong-Rui Chen, Wei-Jie Fu in preparation



Outline

1. Introduction

2. The quark-meson model with functional renormalization group approach

3. Numerical algorithm

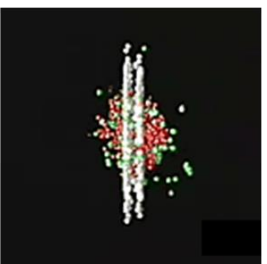
4. Numerical results

5. Sumary

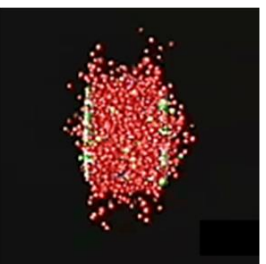
Heavy-ion collision



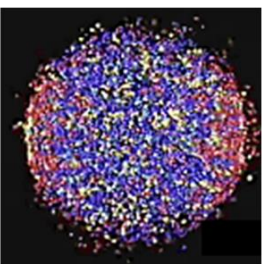
Ions about to collide



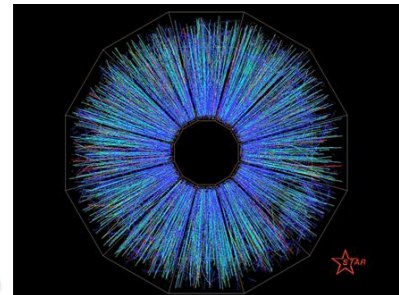
Ion collision



Plasma formation



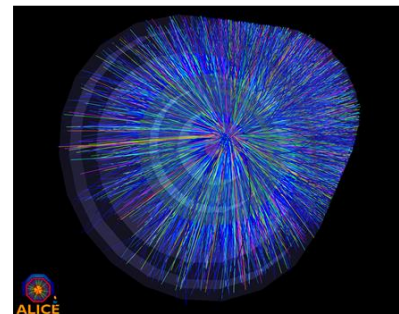
Freeze out



STAR



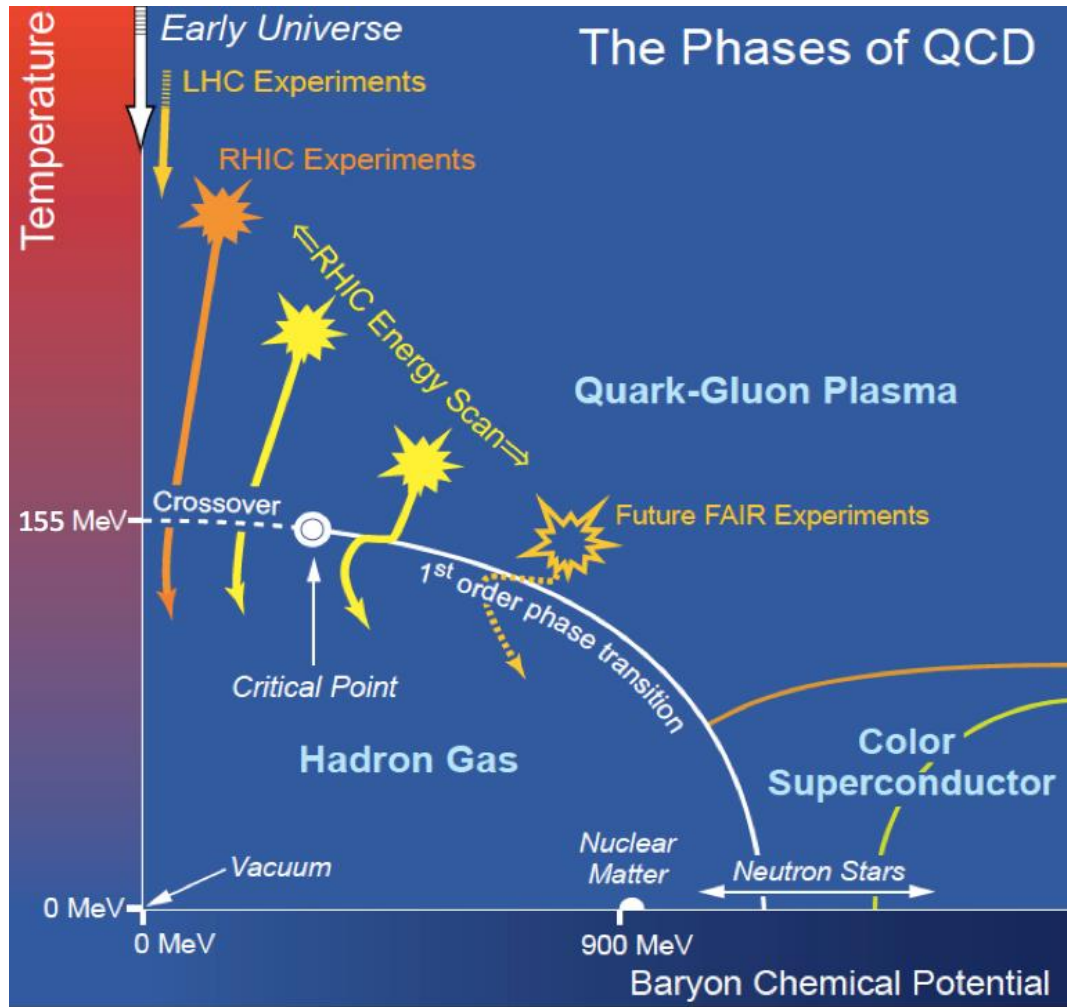
PHENIX



ALICE

What we see

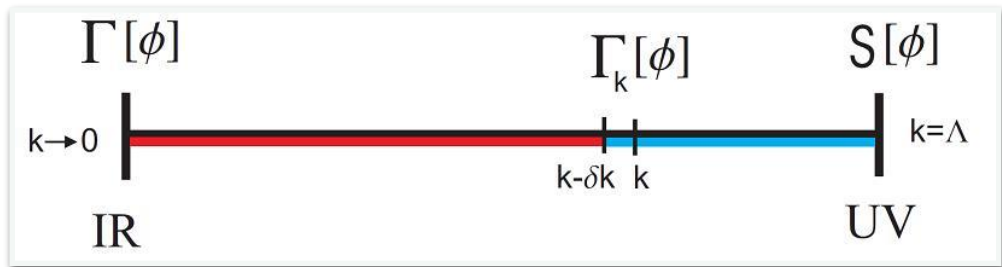
Experiments: Beam Energy Scan



The Hot QCD White Paper (2015)

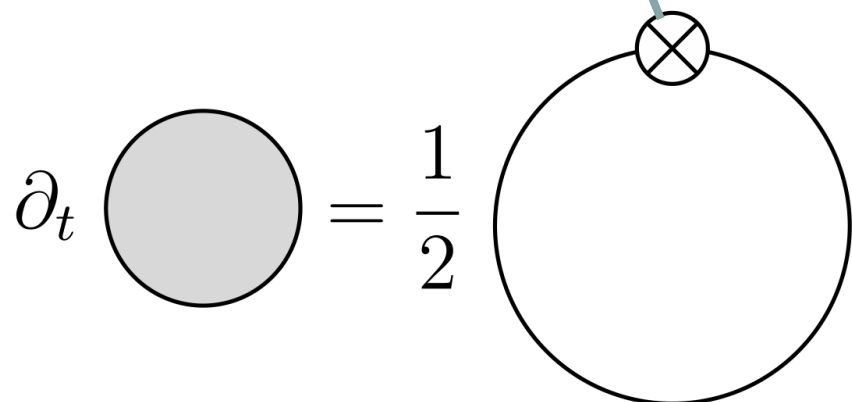
Functional renormalization group

FRG

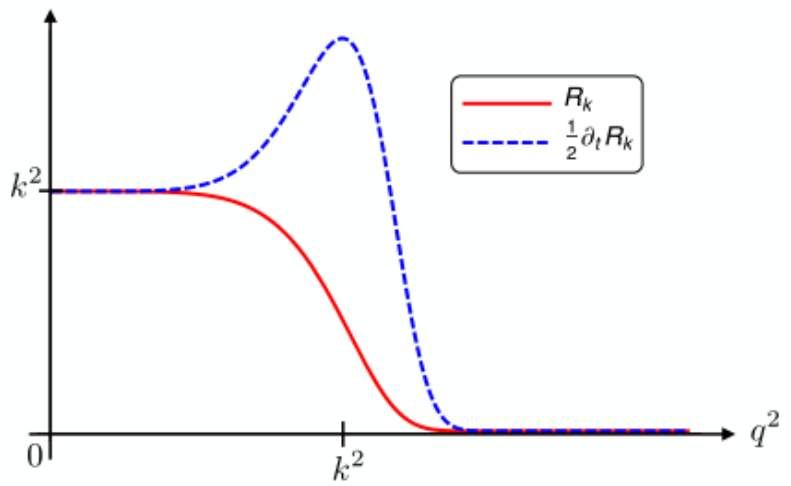


Wetterich equation

$$\partial_t \Gamma_k[\Phi] = \frac{1}{2} STr(G_k \partial_t R_k)$$



$$\partial_t = \frac{1}{2}$$



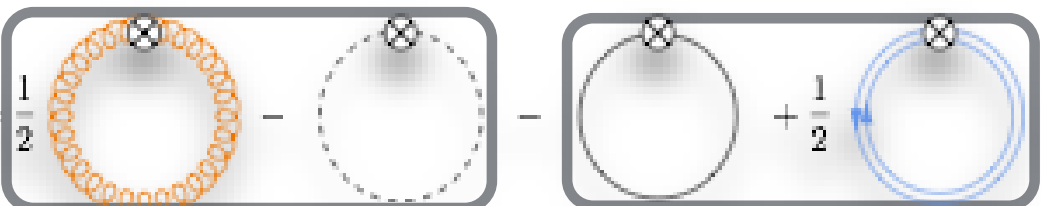
Quark-meson model

The effective action

$$\Gamma_k = \int_x \{ Z_{q,k} \bar{q} (\gamma_\mu \partial_\mu - \gamma_0 \mu) q + \frac{1}{2} Z_{\phi,k} (\partial_\mu \phi)^2 + h_k \bar{q} (T^0 \sigma + i \gamma_5 \vec{T} \cdot \vec{\pi}) q + V_k(\rho) - c \sigma \}$$

The flow equation of effective action

$$\partial_t \Gamma_k[\Phi] = \frac{1}{2} \text{STr} [\partial_t R_k (\Gamma_k^{(2)}[\Phi] + R_k)^{-1}] = \frac{1}{2} \text{Tr}(G_k^{AA}[\Phi] \partial_t R_k^A) - \text{Tr}(G_k^{c\bar{c}}[\Phi] \partial_t R_k^c) - \text{Tr}(G_k^{q\bar{q}}[\Phi] \partial_t R_k^q) + \frac{1}{2} \text{Tr}(G_k^{\phi\phi}[\Phi] \partial_t R_k^\phi)$$



 $\Gamma_{glue,k}[\Phi]$ $\Gamma_{matt,k}[\Phi]$ $\partial_t \Gamma_k[\Phi] = \frac{1}{2} \text{STr} [\partial_t R_k (\Gamma_k^{(2)}[\Phi] + R_k)^{-1}]$
 $= \frac{1}{2} \text{Tr}(G_k^{AA}[\Phi] \partial_t R_k^A) - \text{Tr}(G_k^{c\bar{c}}[\Phi] \partial_t R_k^c)$
 $- \text{Tr}(G_k^{q\bar{q}}[\Phi] \partial_t R_k^q) + \frac{1}{2} \text{Tr}(G_k^{\phi\phi}[\Phi] \partial_t R_k^\phi)$



Flow equation under LPA

under LPA, $\partial_t Z_{\phi/q} = 0$, $\partial_t h = 0$

The flow equation of effective potential:

$$\begin{aligned}\partial_t V_k(T, \mu; \phi) = & \frac{k^5}{12\pi^2} \left[\frac{3}{E_\pi} \coth\left(\frac{E_\pi}{2T}\right) + \frac{1}{E_\sigma} \coth\left(\frac{E_\sigma}{2T}\right) \right. \\ & \left. - \frac{2N_c N_f}{E_q} \left\{ \tanh\left(\frac{E_q - \mu}{2T}\right) + \tanh\left(\frac{E_q + \mu}{2T}\right) \right\} \right]\end{aligned}$$

The flow equation in the vacuum

$$\partial_t V_k(0,0; \phi) = \frac{k^5}{12\pi^2} \left[\frac{3}{E_\pi} + \frac{1}{E_\sigma} - \frac{4N_c N_f}{E_q} \right]$$

B.-J. Schaefer, J. Wambach. Nucl. Phys. A757.2005



Flow equation under beyond LPA

Under beyond LPA, $\partial_t Z_{\phi/q} \neq 0$, $\partial_t h = 0$

The flow equation of effective potential:

$$\begin{aligned}\partial_t V_k(\rho) = & \frac{k^4}{4\pi^2} [(N_f^2 - 1) l_0^{(B,4)}(\bar{m}_{\pi,k}^2, \eta_{\phi,k}; T) + l_0^{(B,4)}(\bar{m}_{\sigma,k}^2, \eta_{\phi,k}; T) \\ & - 4N_c N_f l_0^{(F,4)}(\bar{m}_{q,k}^2, \eta_{q,k}; T, \mu)]\end{aligned}$$

anomalous dimensions

$$\eta_{\phi,k} = -\frac{\partial_t Z_{\phi,k}}{Z_{\phi,k}}$$

$l_0^{(B/F,4)}$ are threshold functions

Wei-jie Fu, Jan M.Pawlowski. Phys.Rev.D.92,116006,2015



Replace variable $\tilde{\rho}$ by a discrete set of points $\tilde{\rho}_i$, $i = 1, 2, \dots n$

$$u_k(\tilde{\rho}) = \sum_{n=0}^{\infty} \frac{1}{n!} u_i^{(n)} (\tilde{\rho} - \tilde{\rho}_i)^n$$

Equating fourth order polynomial expansions of $u'_k(\tilde{\rho})$ around two neighbouring points $\tilde{\rho}_i$ and $\tilde{\rho}_{i+1}$ at half-distance

$$\begin{aligned} (u'_k)_i \left(\frac{\tilde{\rho}_i + \tilde{\rho}_{i+1}}{2} \right) &\equiv u_i^{(1)} + u_i^{(2)} \frac{\tilde{\rho}_{i+1} - \tilde{\rho}_i}{2} + u_i^{(3)} \frac{(\tilde{\rho}_{i+1} - \tilde{\rho}_i)^2}{8} + u_i^{(4)} \frac{(\tilde{\rho}_{i+1} - \tilde{\rho}_i)^3}{48} \\ &= (u'_k)_{i+1} \left(\frac{\tilde{\rho}_i + \tilde{\rho}_{i+1}}{2} \right) \\ &\equiv u_{i+1}^{(1)} - u_{i+1}^{(2)} \frac{\tilde{\rho}_{i+1} - \tilde{\rho}_i}{2} + u_{i+1}^{(3)} \frac{(\tilde{\rho}_{i+1} - \tilde{\rho}_i)^2}{8} - u_{i+1}^{(4)} \frac{(\tilde{\rho}_{i+1} - \tilde{\rho}_i)^3}{48} \end{aligned}$$



Similary for $u''_k(\tilde{\rho})$

$$\begin{aligned}(u''_k)_i \left(\frac{\tilde{\rho}_i + \tilde{\rho}_{i+1}}{2} \right) &\equiv u_i^{(2)} + u_i^{(3)} \frac{\tilde{\rho}_{i+1} - \tilde{\rho}_i}{2} + u_i^{(4)} \frac{(\tilde{\rho}_{i+1} - \tilde{\rho}_i)^2}{8} \\&= (u''_k)_{i+1} \left(\frac{\tilde{\rho}_i + \tilde{\rho}_{i+1}}{2} \right) \equiv u_{i+1}^{(2)} + u_{i+1}^{(3)} \frac{\tilde{\rho}_{i+1} - \tilde{\rho}_i}{2} + u_{i+1}^{(4)} \frac{(\tilde{\rho}_{i+1} - \tilde{\rho}_i)^2}{8}\end{aligned}$$

For the initial and end points

$$\begin{aligned}(u'''_k)_1 \left(\frac{\tilde{\rho}_1 + \tilde{\rho}_2}{2} \right) &\equiv u_1^{(3)} + u_1^{(4)} \frac{\tilde{\rho}_2 - \tilde{\rho}_1}{2} \\&= (u'''_k)_2 \left(\frac{\tilde{\rho}_1 + \tilde{\rho}_2}{2} \right) \equiv u_2^{(3)} - u_2^{(4)} \frac{\tilde{\rho}_2 - \tilde{\rho}_1}{2}\end{aligned}$$

J.Adams, *et al.* Mod. Phys. Lett. 1995,A(10)



Initial condition

The tree-level parameterization of the symmetry potential:

$$V_\Lambda(\phi^2) = \frac{\lambda}{4}(\phi^2) - \frac{\lambda}{2}\phi_0^2\phi^2|_\Lambda$$

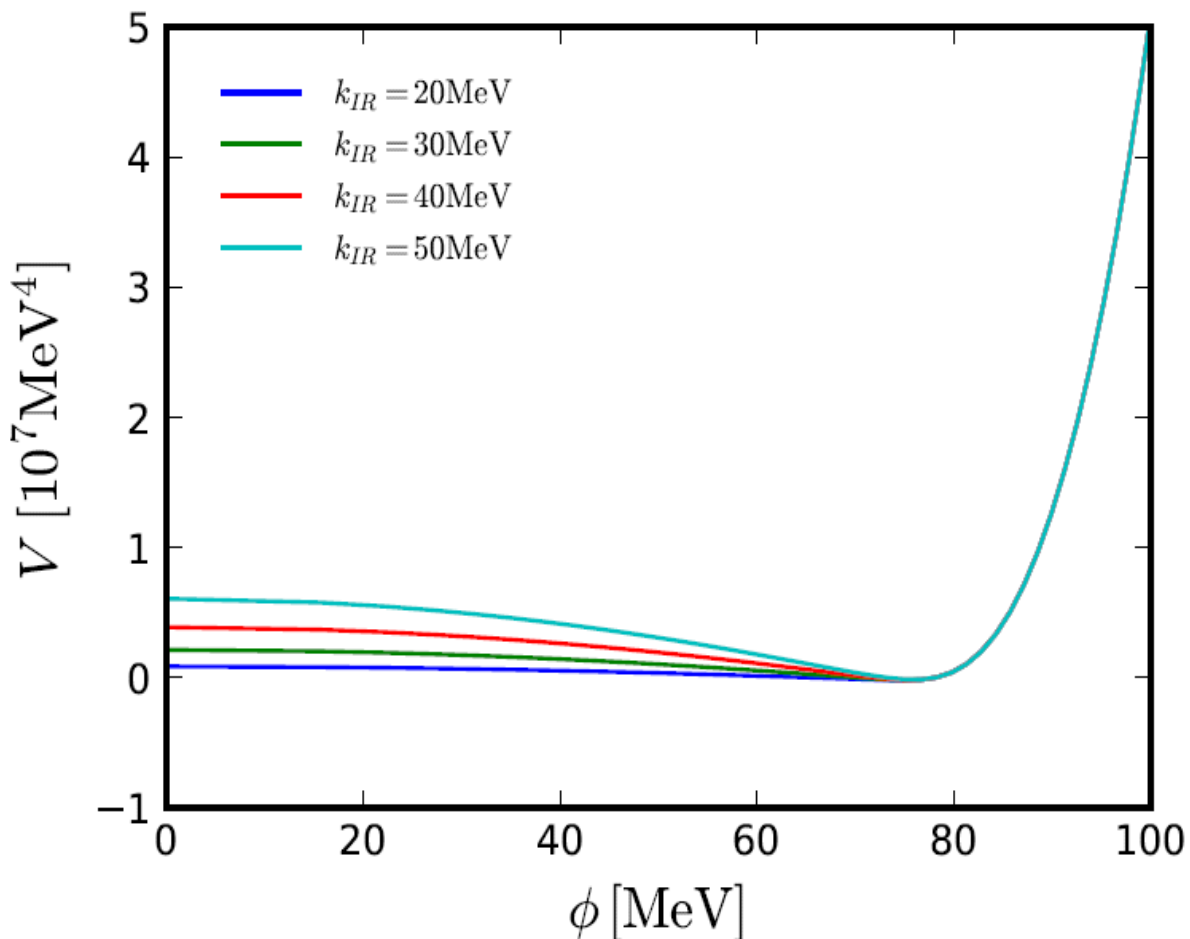
$\Lambda = 500\text{MeV}$, $\lambda = 10$ (LPA) and 8.65 (beyond LPA), $\phi_0^2=0$

The number of grid points is 80 for ϕ between 0~100.

Yukawa coupling $\hbar = 3.2$

Vacuum pion decay constant $f_\pi \sim 87\text{MeV}$

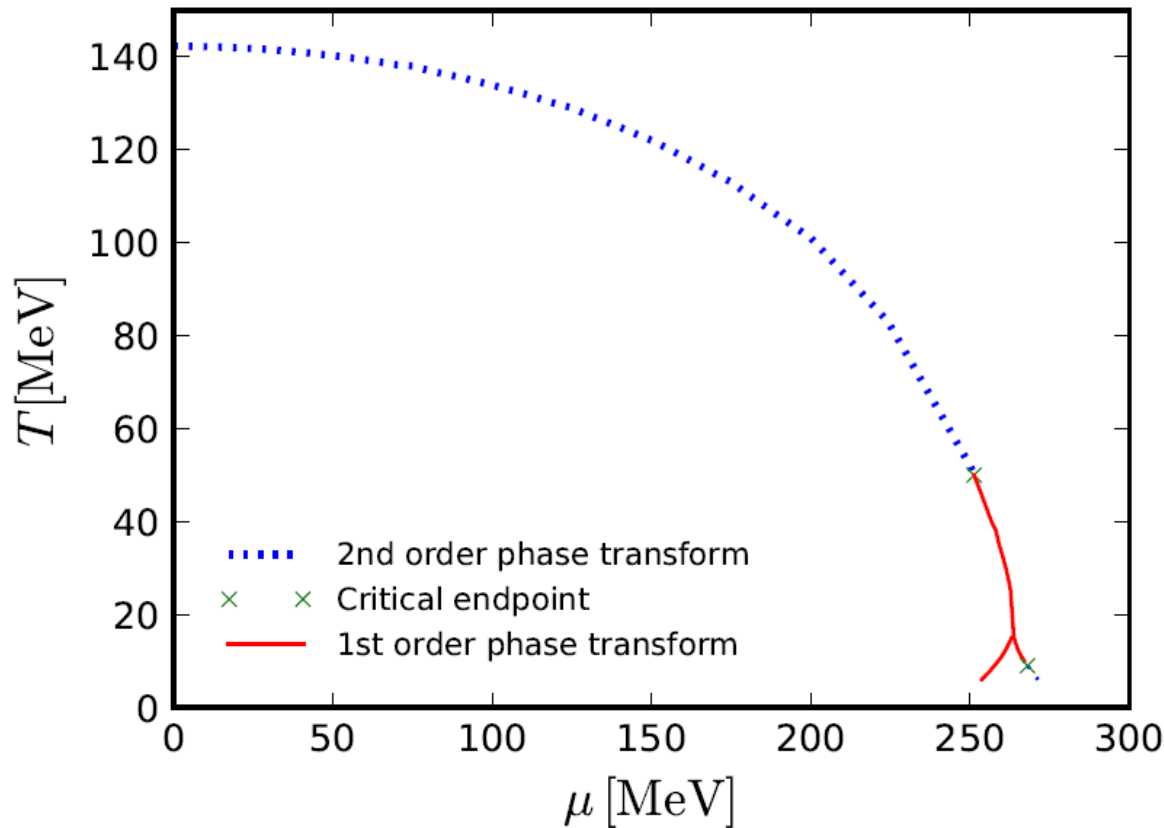
The scale evolution of the potential



The potential becomes flat below the minimum and scale independent above.

The scale evolution barely effects the minimum.

QCD diagram under LPA

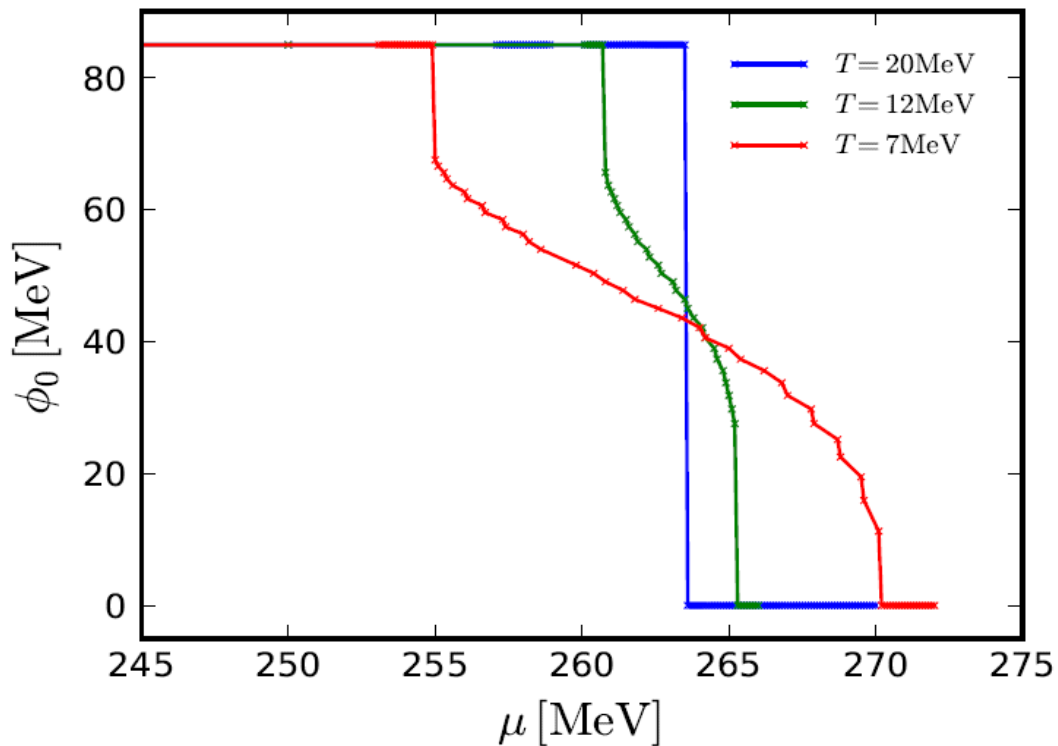


$\mu = 0$, critical temperature of 2nd order phase transition $T_c \sim 143$ MeV

critical endpoint: $T_{c,tri} = 51$ MeV, $\mu_{c,tri} = 250.6$ MeV

$T < 17$ MeV, the single 1st order phase transition splits into two phase transitions

Order parameter versus chemical potential

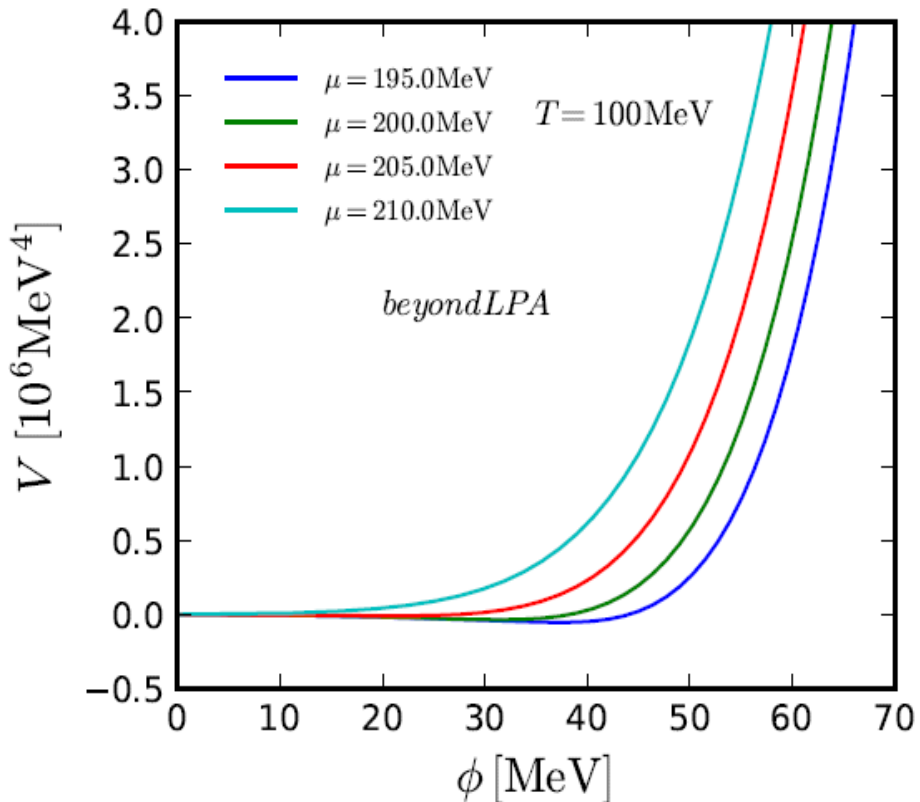
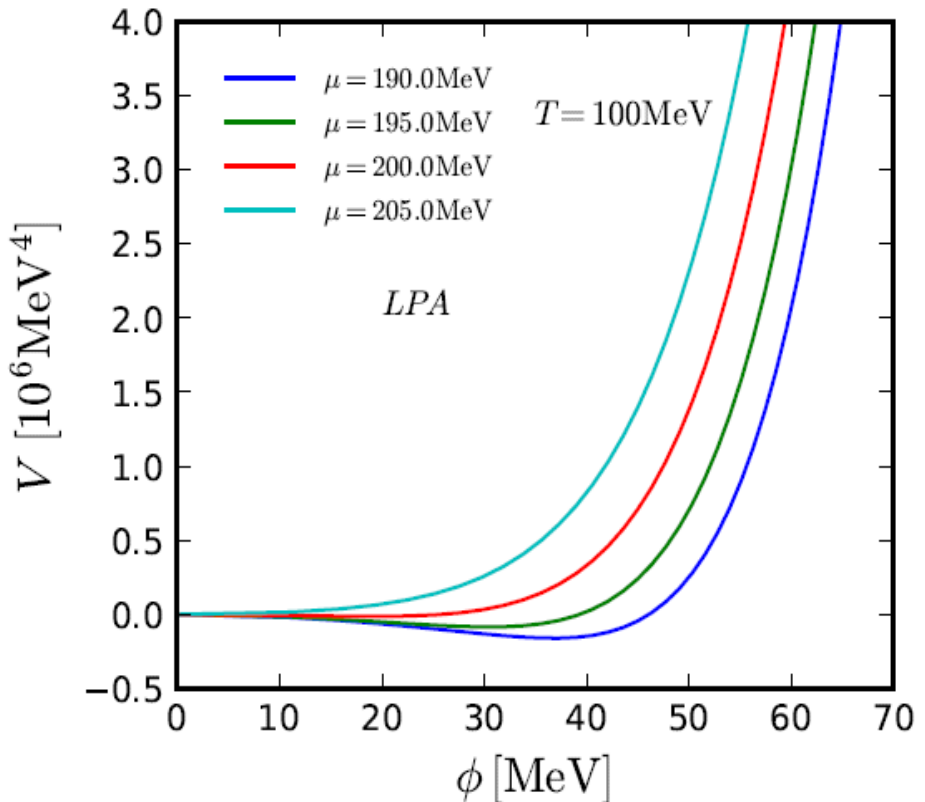


$T=20\text{ MeV}$, order parameter jump to zero after 1st phase transition

$T=12\text{ MeV}$, two gaps in the order parameter corresponding to two phase transitions

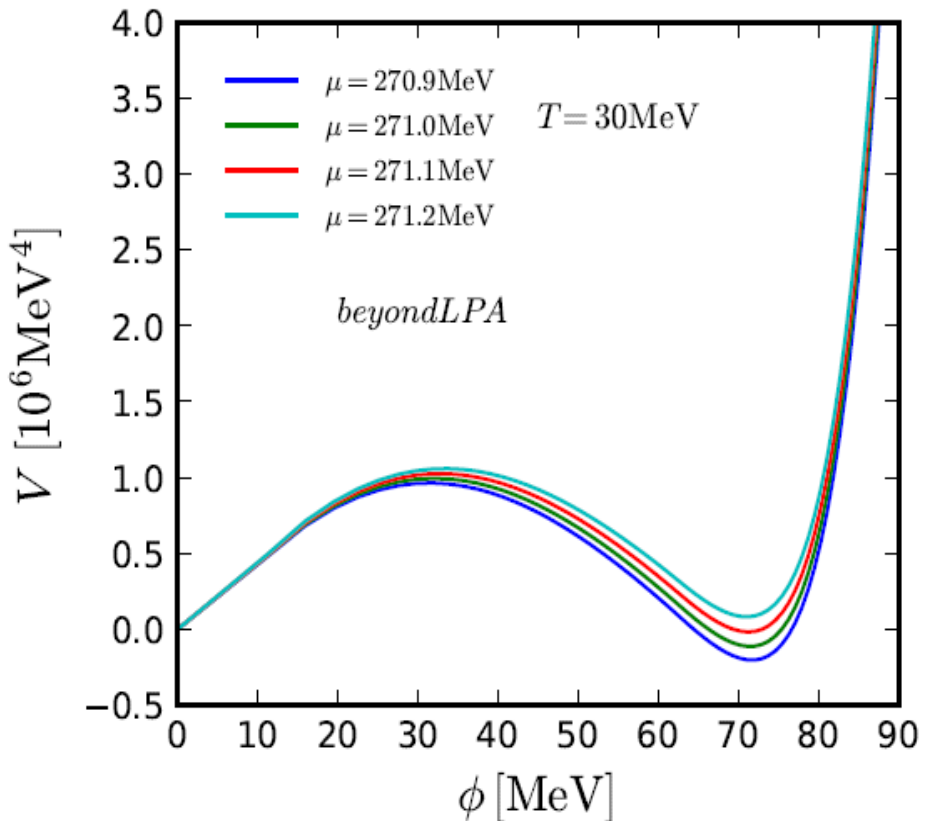
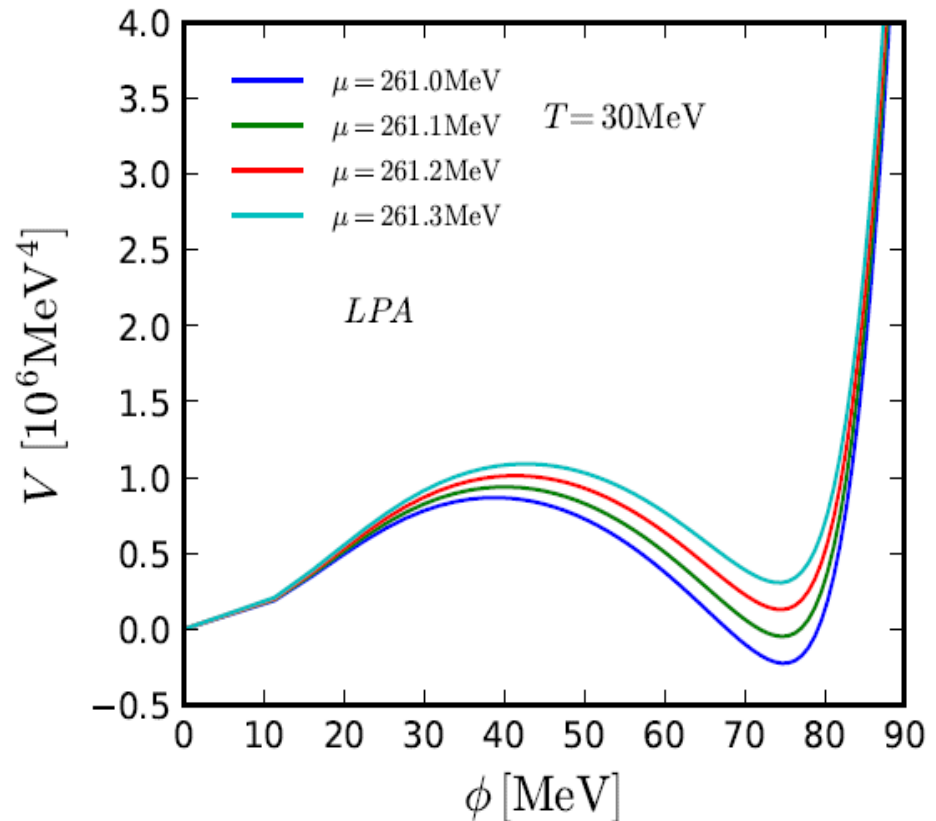
$T=7\text{ MeV}$, order parameter smoothly decreases to zero after the first transition

Phase structure of the effective potential



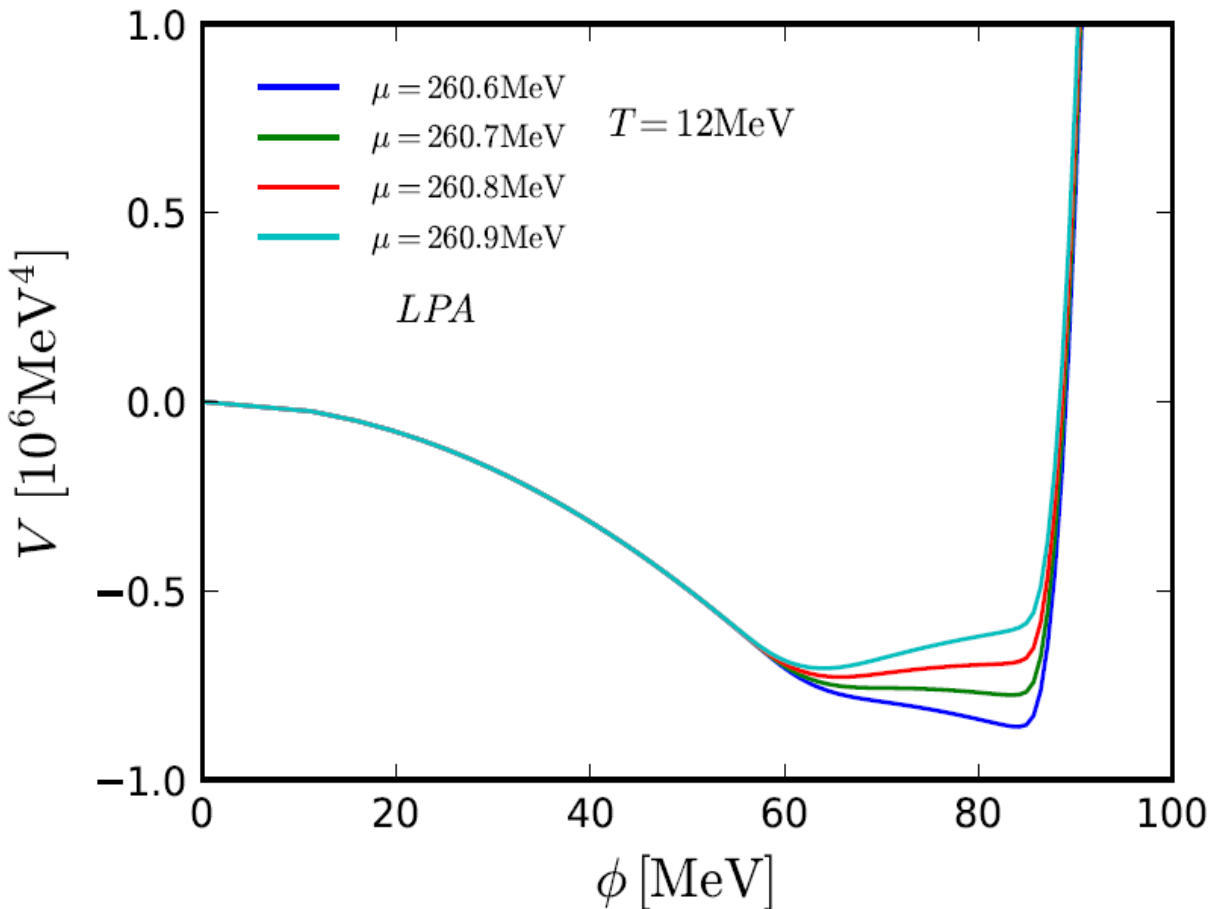
For a second order phase transition, the effective potential only have one (global) minimum.

Phase structure of the effective potential



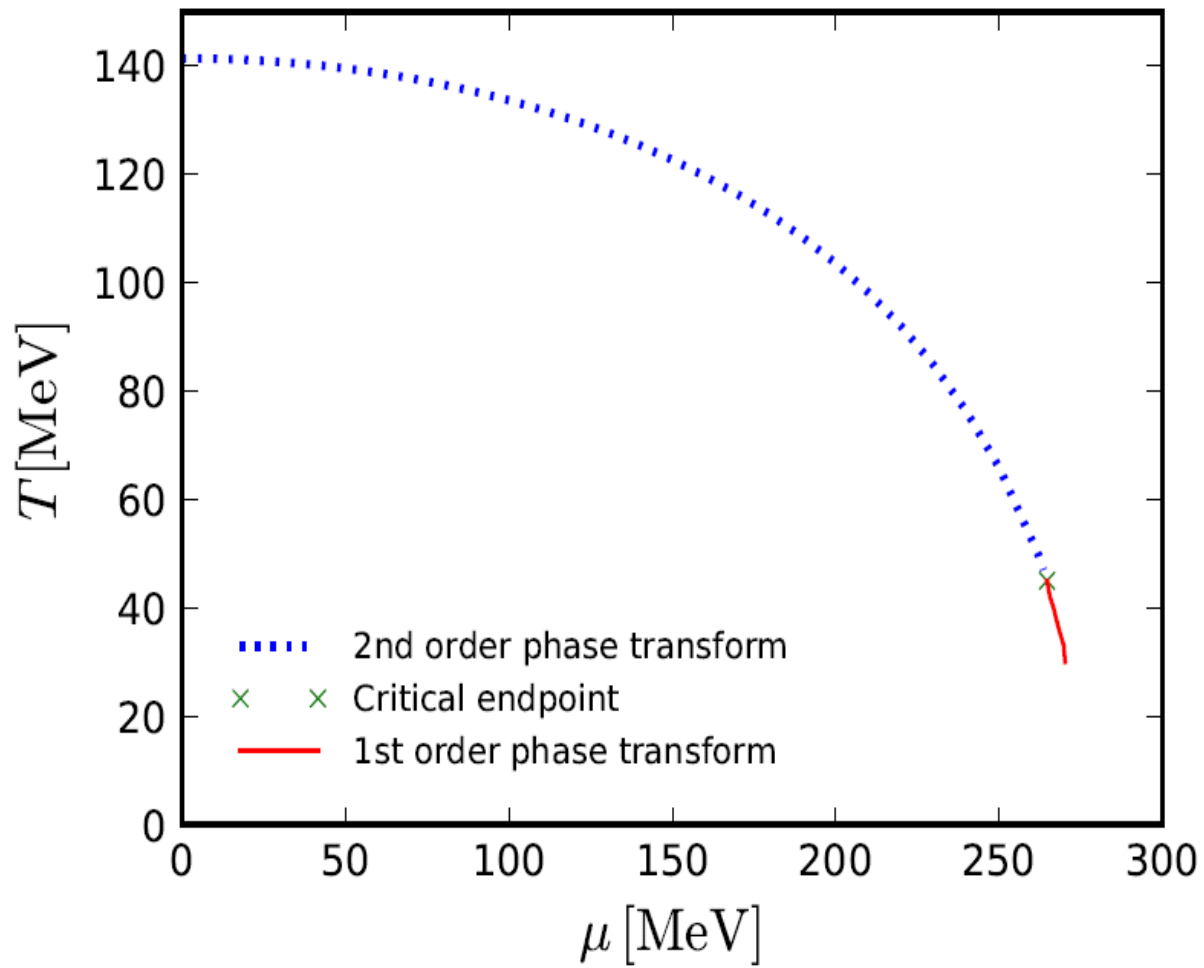
A second minimum at the origin emerges and the global minimum jumps to zero for large chemical potential

Phase structure of the effective potential



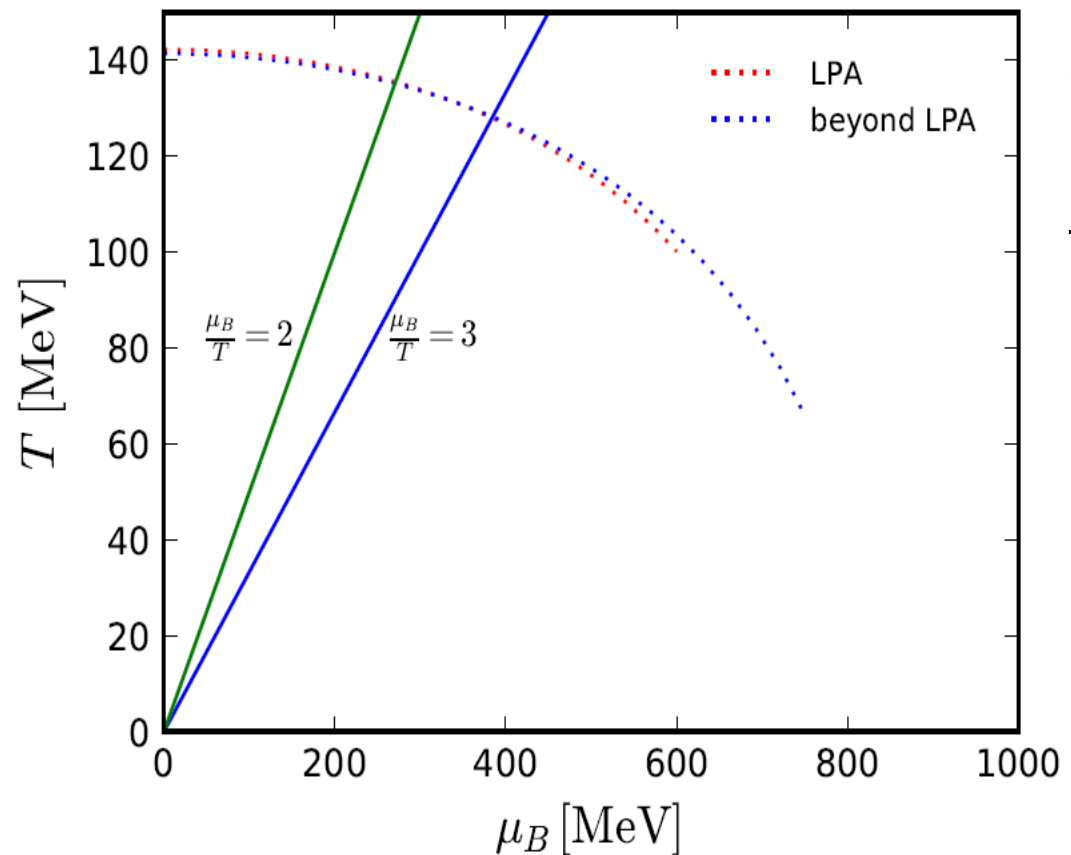
Below the splitting point, the effective potential exhibits two finite minima and is not exactly convex.

Beyond LPA



$\mu = 0$, critical temperature of 2nd order phase transition $T_c \sim 142$ MeV
critical endpoint: $T_{c,tri} = 47$ MeV, $\mu_{c,tri} = 263.6$ MeV

Curvature of phase diagram



The curvature of the phase boundary

$$\frac{T_c(\mu_B)}{T_c} = 1 - \kappa \left(\frac{\mu_B}{T_c} \right)^2 + \lambda \left(\frac{\mu_B}{T_c} \right)^4 + \dots$$

κ

LPA	0.01244 ± 0.00004
beyond LPA	0.01153 ± 0.00003



Summary

- 1) The location of the tricritical point, QCD phase diagram, structure of effective potential is obtained under LPA and beyond LPA.
- 2) For $\mu < \mu_c$, a first-order transition splits into two phase transition for temperature below 17 MeV under LPA.
- 3) The characteristics of order parameter under different phase transition is studied.
- 4) The curvature of phase diagram is calculated.



Thanks for your
attentions!